Journal of ELECTRONIC MATERIALS, Vol. 47, No. 5, 2018
https://doi.org/10.1007/s11664-018-6149-1

Silver Oxalate Ink with Low Sintering Temperature and Good Electrical Property

WENDONG YANG,[1] CHANGHAI WANG,[1,3] and VALERIA ARRIGHI[2]

1.—Institute of Sensors, Signals and Systems, School of Engineering and Physical Sciences, Heriot-Watt University, Edinburgh EH14 4AS, UK. 2.—Institute of Chemical Sciences, School of Engineering and Physical Sciences, Heriot-Watt University, Edinburgh EH14 4AS, UK. 3.—e-mail: C.Wang@hw.ac.uk

Favorable conductivity at low temperature is desirable for flexible electronics technology, where formulation of a suitable ink material is very critical. In this paper, a type of silver organic decomposable ink (10 wt.% silver content) was formulated by using as-prepared silver oxalate and butylamine, producing silver films with good uniformity and conductivity on a polyimide substrate after sintering below 130°C (15.72 $\mu\Omega$ cm) and even at 100°C (36.29 $\mu\Omega$ cm). Silver oxalate powder with good properties and an appropriate solid amine complex with lower decomposition temperature were synthesized, both differing from those reported in the literature. The influence of the factors on the electrical properties of the produced silver films such as sintering temperature and time was studied in detail and the relationship between them was demonstrated.

Key words: Silver, conductive ink, electrical properties, microstructure, film

INTRODUCTION

In recent years, there has been growing interest in the development of low-cost metal conductive inks for flexible electronics. Such inks can be utilized in a variety of applications such as circuit boards,[1] RFID tags,[2] solar cells,[3] thin film transistors,[4] transparent conductive electrodes,[5] flexible displays and electrochemical energy storage systems.[6–8] So far, silver-based inks have been widely developed due to their excellent electrical performance and favorable anti-oxidation property.[9–25] Silver-organic inks, also known as particle-free inks, have been under significant development as there is no aggregation issue associated with such inks during their preparation, storage and patterning process in comparison with other silver-based inks, which is a key advantage. In general, this type of ink is composed of an organic silver precursor and a volatile organic solvent which provide the essential rheological properties for film formation.

(Received October 24, 2017; accepted February 14, 2018; published online February 26, 2018)

Up to now, several types of organic silver precursors have been chosen to formulate silver organic inks that can produce favorable conductivity at low temperature on polymer or paper substrates.[13–24] Overall, each precursor has its merits and drawbacks. For instance, silver neodecanoate,[22] silver nitrate,[16] silver acetate[13] and silver carbonate[14] have a relatively high decomposition temperature (> 200°C) and the last three are also not stable and they can easily decompose in the presence of light. 2-[2-(2-methoxyethoxy)ethoxy] acetate silver,[23] silver hexafluoroacetylacetonate cyclooctadiene[24] and β-ketocarboxylate silver[15] are stable but the synthesis is complex. Therefore, it is still necessary to develop organic silver precursors that can be easily prepared in order to produce silver inks with favorable conductive properties at low sintering temperatures on various flexible substrates.

Silver oxalate is an ideal precursor material for organic silver ink as it has the highest silver content among the above-mentioned silver carboxylates, a low decomposition temperature and can be easily prepared. However, there is only one report in the literature using this material as an ink precursor. Dong et al. synthesized their ink using silver

oxalate as a precursor and ethylamine as the complexing agent.[17] The silver film sintered at 170°C for 30 min had a resistivity of 8.4 $\mu\Omega$ cm. Although interesting results have been obtained in this case, the developed ink is still not ideal and some improvement is needed. Firstly, the silver oxalate decomposition depends on the preparation method.[27,28] Dong et al. only investigated one approach to prepare the silver oxalate powder which gives a relatively high decomposition temperature (210°C). Different methods or procedures should be studied to produce silver oxalate powders with a lower thermal decomposition temperature, which is beneficial to the subsequent ink property.[28] Secondly, only one kind of amine, ethylamine, was used as the ink complexing agent. It is well known that the type of amine is a key factor in determining the thermal decomposition temperature of the silver complex in the ink.[26] Appropriate amine complexes which could significantly decrease the sintering temperature and make inks usable on plastic substrates need to be investigated. Thirdly, the reaction mechanisms in ink formulation and the metallization process based on such a material have not been studied in detail. Lastly, the ink sintering temperature in that case for obtaining a better electrical performance, 170°C, is still high for an application with some low-cost polymer based on flexible substrates such as polyethylene terephthalate. Therefore, it is necessary to develop a silver oxalate ink that can produce silver film with favorable conductive properties below 170°C and to elucidate its formulation mechanism.

In this paper, a decomposable silver organic ink was formulated in a mixed organic solvent via a complexing process of the as-prepared silver oxalate and butylamine. The resultant silver films have shown favorable conductivity on a polyimide substrate after sintering at 130°C, and even at temperatures as low as 100°C. Silver oxalate powders with good properties were prepared by using a method differing from the existing reports. The physical phase, chemical composition and thermal behavior have been studied. The effect of changing the amine compound on the thermal properties of the formulated ink was investigated. The chemical reactions occurring within the ink and the film formation process were studied. Surprisingly, a solid silver amine complex was found. The effects of sintering temperature and time on the microstructure and electrical properties of the silver films prepared from the inks were also investigated in detail.

EXPERIMENTAL

Materials

Silver nitrate ($AgNO_3$), oxalic acid ($H_2C_2O_4$), sodium hydroxide (NaOH), ethylenediamine ($C_2H_8N_2$), 1, 2-diaminopropane ($C_3H_{10}N_2$), butylamine ($C_4H_{11}N$), ethylene glycol ($C_2O_2H_6$) and ethanol (C_2H_6O) were purchased from Sigma-Aldrich and were used as received without further purification. Polyimide films (PI) used as substrates in this study was obtained from DuPont (Kapton 500 HN, 127 μm in thickness). Before application, 15 mm × 15 mm PI samples were cleaned with deionized water and ethanol, and then dried.

Synthesis

The silver organic inks used in this study were prepared in organic solvents using silver oxalate and butylamine. Silver oxalate was synthesized as follows: oxalic acid (0.45 g) and sodium hydroxide (0.4 g) were first each dissolved in 10 ml of deionized water, then the solutions were mixed and stirred for 30 min at room temperature. Then, 10 ml of silver nitrate solution (1.7 g $AgNO_3$) was added to the above mixture. After 1 h of stirring in the absence of light, the product was collected by vacuum filtration and washed with water three times and with ethanol twice, dried at 40°C for 8 h in an oven and stored both away from light. The obtained silver oxalate powder was about 1.440 g in weight.

For ink preparation, 0.152 g of the obtained silver oxalate was dispersed in 0.75 ml of a mixed solvent containing ethanol (0.375 ml) and ethylene glycol (0.375 ml). After stirring for 5 min, butylamine (0.192 ml) was added. The mixture was stirred for 60 min to form the ink. The appearance of the solution changed during this period, from the initial suspension to a homogeneous transparent solution. The silver content in the ink was about 10 wt.%.

Ink Deposition and Sintering

The as-prepared ink was dropped on the PI films, and sintered at selected temperatures for up to 60 min. The film thickness was controlled by the volume of ink solution deposited onto the PI film.

Characterization

The thermal behaviors of the powder and ink were investigated by differential scanning calorimetry (DSC; TA instrument) at a heating rate of 10°C/min from room temperature to 250°C and a nitrogen flow rate of 80 ml/min. Ultraviolet–visible (UV–Vis) absorption spectra were obtained on a Lambda 25 UV–Vis spectrophotometer using water as solvent. Fourier transform infrared (FT-IR) spectra in the range of 400–4000 cm^{-1} were recorded on a Thermo Scientific Nicolet iS5 FT-IR spectrometer. X-ray diffraction (XRD) analysis was recorded by using Cu Kα and λ = 0.15418 nm. The sizes of the silver nanocrystallites were calculated using Scherrer's formula. The morphologies of the silver films after sintering were observed on a FEI Quanta 3D Scanning Electron Microscope (SEM). The chemical composition was determined on an Oxford X-maxN 150 surface energy disperse spectrometer (EDX).

The sheet electrical resistivity was measured using a 4-point probe method (Jandel Engineering, UK). The thickness of the sintered films was measured using a Dektak surface profilometer and was used to calculate the equivalent bulk resistivity.

RESULTS AND DISCUSSION

Characterization of Silver Oxalate

Silver oxalate was selected as the silver precursor because it has high silver content (71 wt.% silver) and a simple structure, only producing silver metal and carbon dioxide upon thermal decomposition at a relatively low temperature.[27,28] This is desirable in ink applications on temperature-sensitive substrates. The silver oxalate powder (named S_1) used in this study was prepared through an ion exchange reaction by sodium hydroxide, oxalic acid and silver nitrate as shown below:

$$H_2C_2O_4 + 2NaOH \rightarrow Na_2C_2O_4 + H_2O$$

$$Na_2C_2O_4 + 2AgNO_3 \rightarrow Ag_2C_2O_4 + 2NaNO_3$$

As a key component of the ink, the characteristic of the silver oxalate powder was important since it determines the ink properties such as thermal decomposition behavior. According to the work carried out by Boldyrev et al., silver oxalate decomposition depends upon its preparation method.[27] For the purpose of comparison, another procedure was also employed to obtain silver oxalate powder (named S_2). This involved using only silver nitrate and oxalic acid as the reaction materials.

The thermal behavior of the as-prepared silver oxalate powders, S_1 and S_2, was studied by DSC in N_2 atmosphere using the same parameter. As shown in Fig. 1, the DSC curve of the S_1 powder displays two major endothermic peaks, at 166°C and 185°C, while the S_2 trace gives two peaks, at 224°C and 234°C. All of these peaks are attributed to the decomposition of silver oxalate. The presence of two different peaks in each curve may be related to the size and structure as well as the morphology of the as-prepared powders. Obviously, the decomposition temperature of the S_1 powder is lower than that of S_2, which is a preferred property for the subsequent ink. Therefore, the former preparation method was selected for the following studies.

XRD, FT-IR, TG and SEM/EDX measurements were used to characterize the physical phase, structure, mass change versus temperature, morphology and chemical composition of the S_1 powder.

The TG curve of S_1 powder given in Fig. 2 indicates that the sample starts to decompose at 150°C and a maximum rate of weight loss occurs at 200°C, which is consistent with the DSC results. The total weight loss is about 28 wt.%; the remaining 72 wt.% is in good agreement with the proportion of silver in the silver oxalate (71 wt.%).

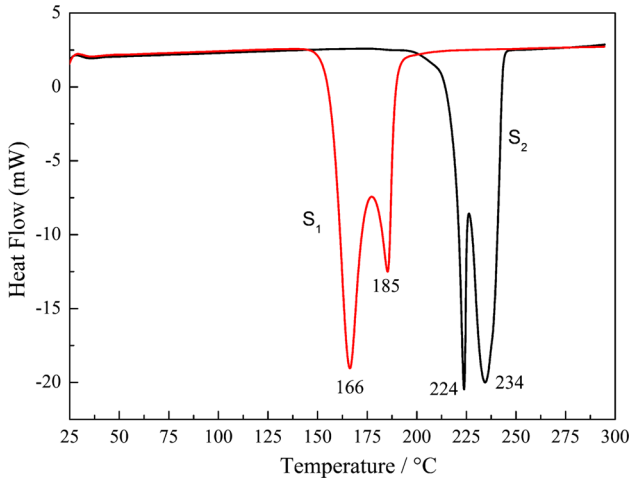

Fig. 1. DSC traces of as-prepared silver oxalate powders. S_1 powder was prepared using sodium hydroxide, oxalic acid, and silver nitrate. S_2 powder was prepared using oxalic acid and silver nitrate.

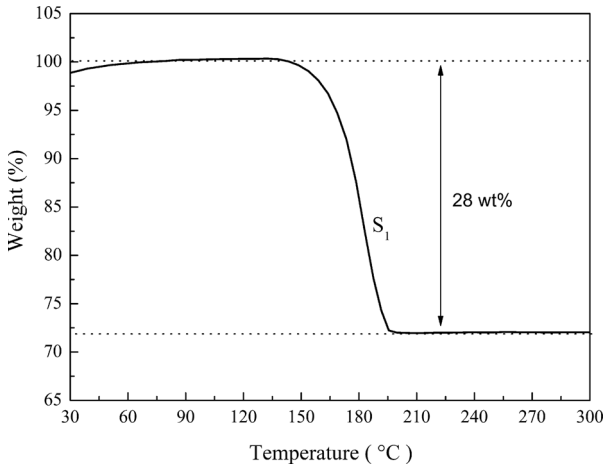

Fig. 2. TG curve of the as-prepared S_1 powder.

Figure 3 shows the XRD pattern of the S_1 powder. The main peaks appeared at 17.17°, 19.07°, 26.48°, 28.76°, 29.8°, 32.14°, 36.43°, 38.74°, 39.49°, 47.05°, 51.56° and 67.60°. The x-ray data are in good agreement with the JCPDS No.022-1335 for silver oxalate. No diffraction peaks from any other impurities were detected, indicating that the reaction was completed and the silver oxalate powder was successfully prepared.

Figure 4 shows the IR spectrum of the S_1 powder. The peak at 1570 cm^{-1} is attributed to the asymmetric stretching vibration of C=O. The peaks at 1380 cm^{-1} and 1300 cm^{-1} are from C=O stretching vibrations. The peaks at 772 cm^{-1} and 519 cm^{-1} arise from vibrations of the metal–O group.[17] These features confirm that silver oxalate has a structure of carboxylates.

The morphology and chemical composition was identified by combined SEM/EDX measurements as shown in Fig. 5. Figure 5a gives the SEM image of

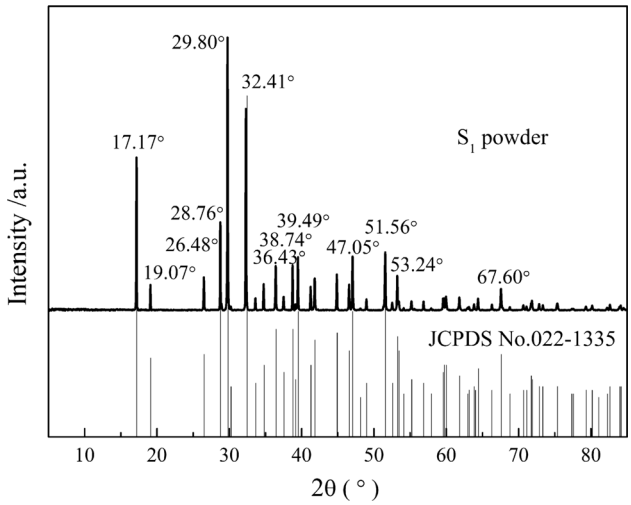

Fig. 3. XRD pattern of S_1 powder.

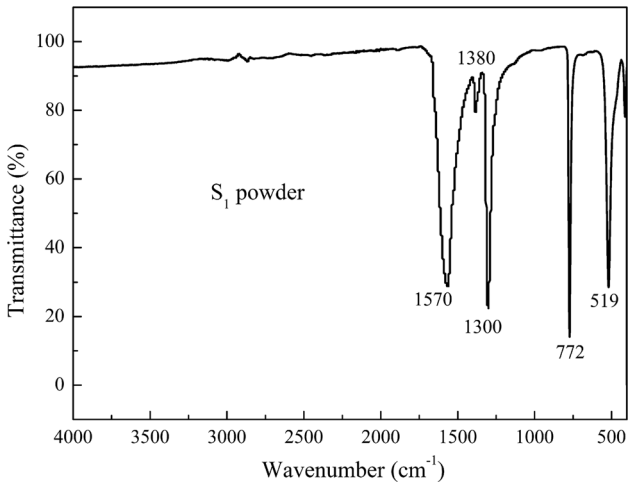

Fig. 4. FT-IR spectrum result of the synthesized S_1 powder.

the as-prepared silver oxalate, which clearly shows a hexagonal columnar morphology with two kinds of particle size. This is in agreement with the DSC results where two peaks were observed. The EDX measurements show that three elements (C, O, and Ag) exist in the powder, as expected from the chemical structure of the compounds.

All the results demonstrate that the prepared S_1 powder is an ideal ink precursor material.

Ink Formulation

The effect of using different amines on the thermal properties of the silver amine complex solution was investigated. The as-prepared solid silver oxalate powder was dissolved in an aqueous solution containing ethylenediamine, 1,2-diaminopropane and butylamine to form the corresponding complex, named solution 2, solution 1 and solution 3, respectively. In order to make a reasonable comparison, the weight of silver oxalate and water were the same in each solution and the Ag/amine molar ratios were kept at a constant value of 1:2.5. The results are given in Fig. 6a. The first peak, around 100°C, is mainly attributed to water evaporation, whereas the peaks at temperatures above 100°C correspond to the thermal decomposition of the silver amine complexes. Clearly, the solution containing butylamine has the lowest decomposition temperature (around 109°C), which is a very desirable feature. Low thermal decomposition temperatures of the silver–amine complex make it possible for the subsequent ink to be sintered at a much lower temperature, which is quite advantageous for patterning conductive features on temperature-sensitive substrates.[26] Therefore, for ink preparation, butylamine, a small molecule with a low boiling point (77°C), was chosen as the ligand to dissolve the silver oxalate in the organic solvents and to decrease the decomposition temperature of the complex. Also, using this type of amine, the sintering process would become faster since a silver–amine complex with less organic content could be formed, requiring less energy and time to evaporate the organic content. Here, the decomposition behavior of the complexes formulated by the S1 and S2 silver oxalate powders and butylamine were also investigated using the DSC instrument, as shown in Fig. 6b. It can be seen that two pf the complexes have similar thermal behaviors while the complex from the S1 powder gives a relatively lower decomposition temperature (138°C), thereby the S1 powder were chosen as the ink precursor material for the following experiments. It should be noted here that the two complexes were found to be present in a solid state, which is different from all the other organic silver complexes that usually exist in liquid form.

Ethanol was used as the solvent and ethylene glycol as a co-solvent to suppress the undesirable coffee ring effect caused by ethanol in the film sintering process.[13]

It was found that the sparingly soluble silver oxalate powder could be easily dissolved in the organic solution containing butylamine, mainly via the following complexing reaction, resulting in a soluble complex, which might exist in the form of molecules of $[Ag(C_4H_{11}N)_2]_2^{2+}$ and $(C_2O_4)^{2-}$ in the organic solvents:

$$Ag_2C_2O_4 + 2C_4H_{11}N \rightarrow \left[Ag(C_4H_{11}N)_2\right]_2C_2O_4$$

FT-IR and ^{1}H-NMR were employed to investigate and confirm this mechanism. For the measurements, the complex sample was prepared using only silver oxalate and butylamine in a stoichiometric ratio. FT-IR and ^{1}H-NMR were used to characterize this complex, and the spectra are shown in Figs. 7 and 8, respectively.

In the spectrum of butylamine, the absorption peaks at 3368 cm^{-1} and 3285 cm^{-1} correspond to

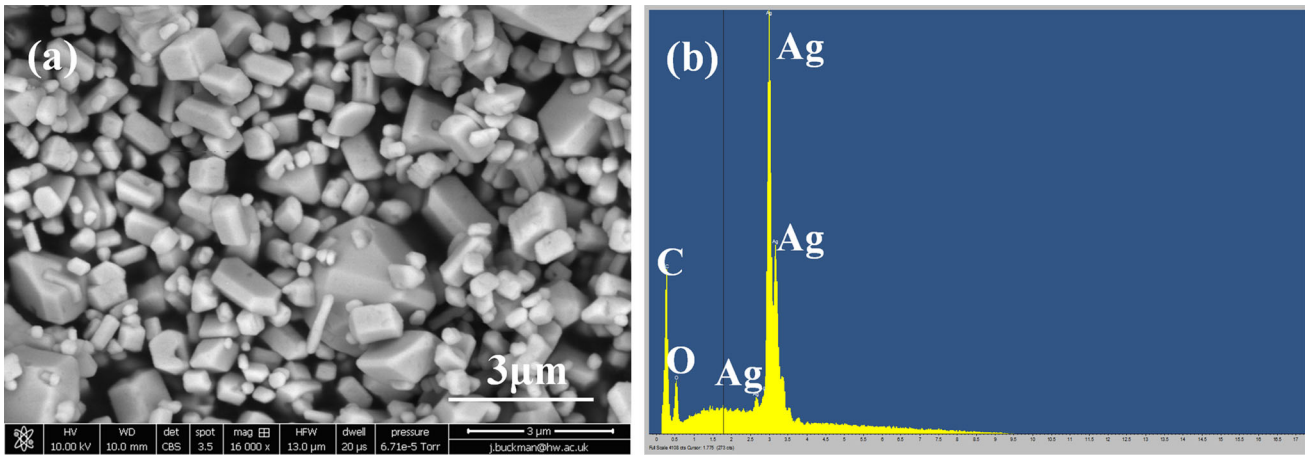

Fig. 5. (a) SEM image of the synthesized S_1 powder. (b) EDX result of the as-prepared S_1 powder.

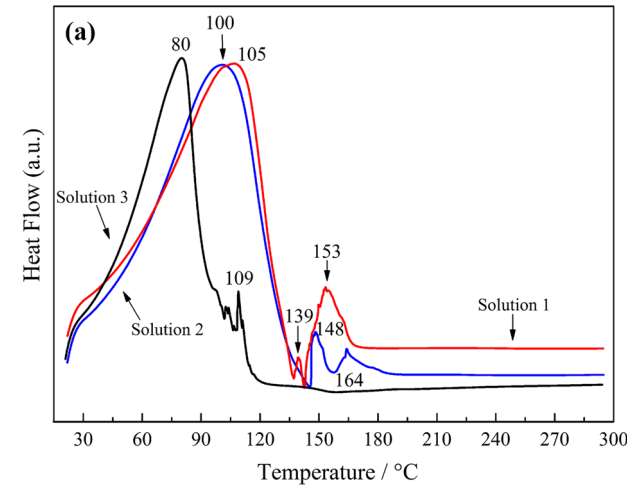

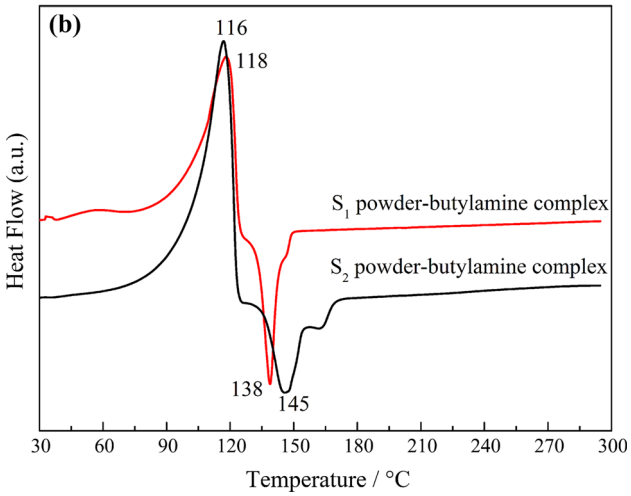

Fig. 6. (a) DSC curves of the silver amine complex solutions formulated with various amines. (b) DSC curves of the silver amine complexes prepared by two silver oxalate powders.

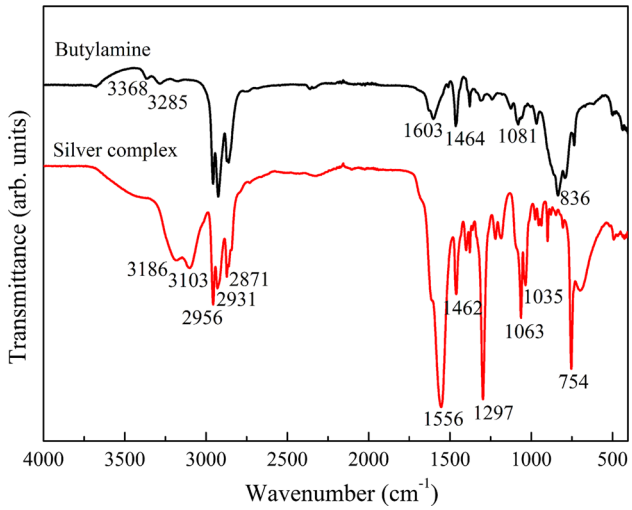

Fig. 7. FT-IR spectra of the butylamine and $[Ag(C_4H_{11}N)_2]_2C_2O_4$ solid complex.

the asymmetric and the symmetric stretch of the NH_2 groups. The two peaks at 2956 cm^{-1} and 2931 cm^{-1} correspond to the asymmetric stretch of CH_3 and CH_2 groups, respectively. The peak at 2865 cm^{-1} relates to the symmetric stretching mode of CH_2. The peaks at 1603 cm^{-1} and 1464 cm^{-1} belong to the scissoring vibration of the NH_2 groups and scissoring vibration of CH_2, respectively. As for the complex, it is worth noting that the peaks associated with NH_2 groups undergo a dramatic red-shift, from 3368 cm^{-1} to 3186 cm^{-1} and 3285 cm^{-1} to 3103 cm^{-1}.The carbonyl peak appears at 1556 cm^{-1}, which is from the silver oxalate. These changes indicate that the butylamine reacts with silver oxalate to form a complex, which donates electrons from the amino group to the silver atoms, decreasing the electron density of the amino groups

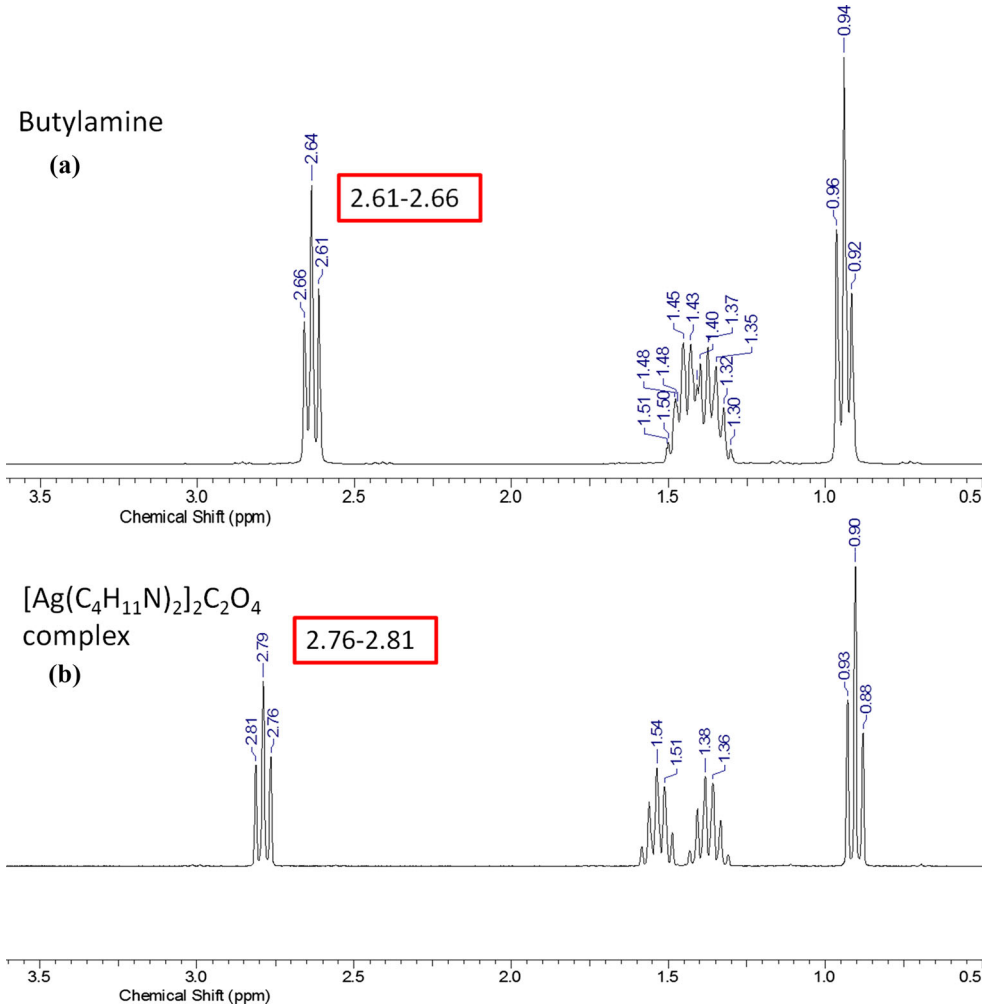

Fig. 8. (a) ^{1}HNMR spectrum of butylamine. (b) ^{1}HNMR spectrum of solid $[Ag(C_4H_{11}N)_2]_2C_2O_4$ complex. D_2O solvent for both.

and therefore resulting in a red-shift of the NH_2 stretching peak.

The ^{1}H-NMR results of the butylamine and the solid $[Ag(C_4H_{11}N)_2]_2C_2O_4$ complex in Fig. 8 also confirm this reaction process. The chemical shift changes of CH_2 connected to NH_2 are very significant, from 2.61–2.66 to 2.76–2.81, indicating the formation of the complex.

Ink Thermal Behavior

DSC analysis was carried out to investigate the temperature window for thermal decomposition of the as-prepared ink.

As shown in Fig. 9, there are three peaks on the DSC curve of the silver ink. The first peak at 100°C is likely due to evaporation of unreacted amine and ethanol in the ink. The second peak at 117°C is attributed to the decomposition of the silver complex whereas the third peak at 140°C might be from evaporation of ethylene glycol and coalescence of silver nanoparticles produced.[26] It should be noted that the decomposition temperature of the as-prepared ink is much lower than the that of the silver oxalate powder. This is most probably because the lone pair electrons in nitrogen of butylamine can

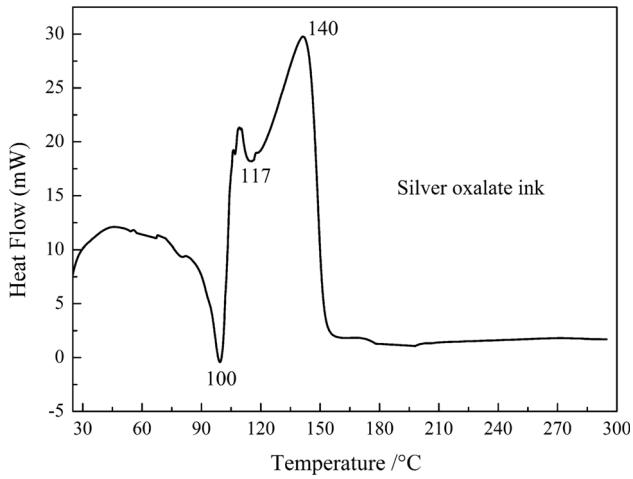

Fig. 9. DSC curve of the as-prepared ink.

effectively combine with the silver ion to form a silver-amine complex with a lower redox potential, which reduces the decomposition temperature.[21] This is similar to the thermal behavior of other silver salt-based inks.[17,26]

UV–Vis absorption data are sensitive to the size of the metal nanoparticles, especially for silver nanoparticles.[29] Therefore, UV–Vis spectroscopy was used to investigate the temperature-dependent absorption characteristics of the ink, as shown in Fig. 10. For samples prepared at temperatures below 115°C, no absorption peak can be seen in the UV spectra. However, when for ink is heated above 115°C, an absorption peak appears around 315 nm. As silver atoms absorb in the 250–330 nm region, this peak is associated with the formation of Ag^0.[28] In other words, the $[Ag(C_4H_{11}N)_2]_2C_2O_4$ is decomposed into elemental Ag.

Based on the results discussed so far, it can be concluded that, during heating, solvent evaporation occurs, followed by decomposition of the silver complex at elevated temperatures.

Effect of Sintering Temperature on Microstructure of Silver Films

Silver films were prepared by the ink drop-coating method on the cleaned PI substrates. The sintering process was carried out on a hotplate in a chamber. According to the DSC results and UV–Vis analysis of the ink, temperatures between 100°C and 160°C were chosen for thermal sintering.

Figure 11 gives an optical image of the as-prepared silver ink and the surface profile of a silver film after sintering. It can be seen that the thickness of the sintered silver film was about 1.3 ± 0.3 μm. As expected, the film has a continuous surface without suffering from the coffee ring effect.

X-ray diffraction was used to probe the crystalline structure of the silver films obtained by sintering at different temperatures for 60 min (Fig. 12). The data are in agreement with the values for a face-centered cubic (fcc) crystal structure of silver. The peaks at 38.2°, 44.4°, 64.5°, 77.5° and 81.6° correspond to the (111), (200), (220), and (311) crystal planes of Ag NPs, respectively, and were the same in all the films. No diffraction peaks from any other impurities were detected, revealing the formation of well-crystallized silver films.

$$[Ag(C_4H_{11}N)_2]_2C_2O_4 \rightarrow Ag(s) + C_4H_{11}N(g) + CO_2(g)$$

It should be noted that $[Ag(C_4H_{11}N)_2]_2C_2O_4$ can transform to silver crystals at 100°C, which is a key advantage of the ink developed in this work.

The crystallite sizes of the silver nanoparticles in the films formed at 100°C, 130°C and 160°C were determined from the XRD data (Debye–Scherrer equation). The results are given in Table I.

Clearly, the crystallite sizes of the silver nanoparticles in the film increases gradually with increasing

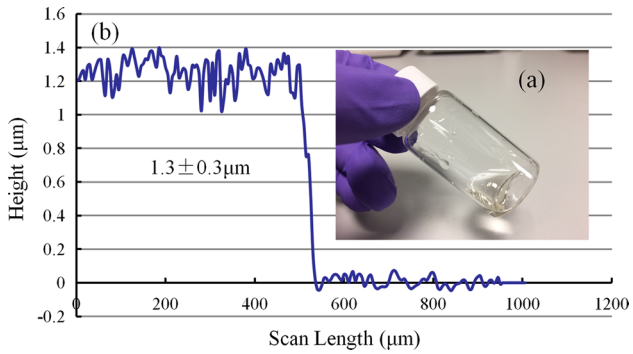

Fig. 11. (a) As-prepared silver ink; (b) surface profile of a sintered silver film (130°C, 60 min).

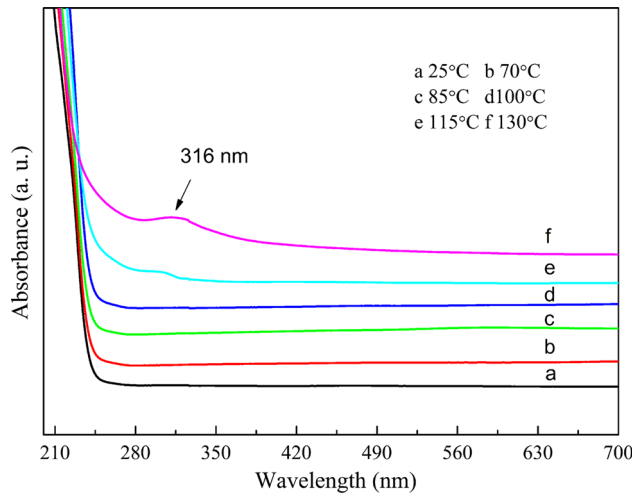

Fig. 10. UV-Vis absorption spectra of silver citrate ink at different heating temperatures.

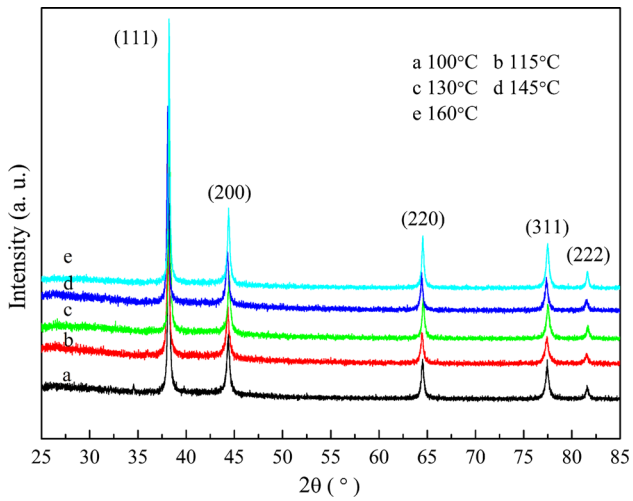

Fig. 12. XRD patterns of the silver films obtained at different sintering temperatures for 60 min. Data shifted vertically, for clarity.

Table I. Particle sizes of silver nanocrystals in the film at different sintering temperatures

Sintering temperature (°C)	2θ (°)	FWHM	Size (nm)
100	38.211	0.237	35.125
130	38.286	0.222	35.433
160	38.231	0.199	41.835

temperature, from 35.125 nm to 41.835 nm. This can be ascribed to the nucleation and growth of the silver grains. It is known that nucleation of silver particles occurs in the initial stage of sintering followed by subsequent grain growth.[17] The higher the sintering temperature, the larger the crystallite size since a large number of crystal nuclei would form, followed by a fast growth. For sintering at high temperature (160°C), solvent evaporation is fast, which enables fast growth of silver nanocrystals, thereby resulting in a relatively large size.

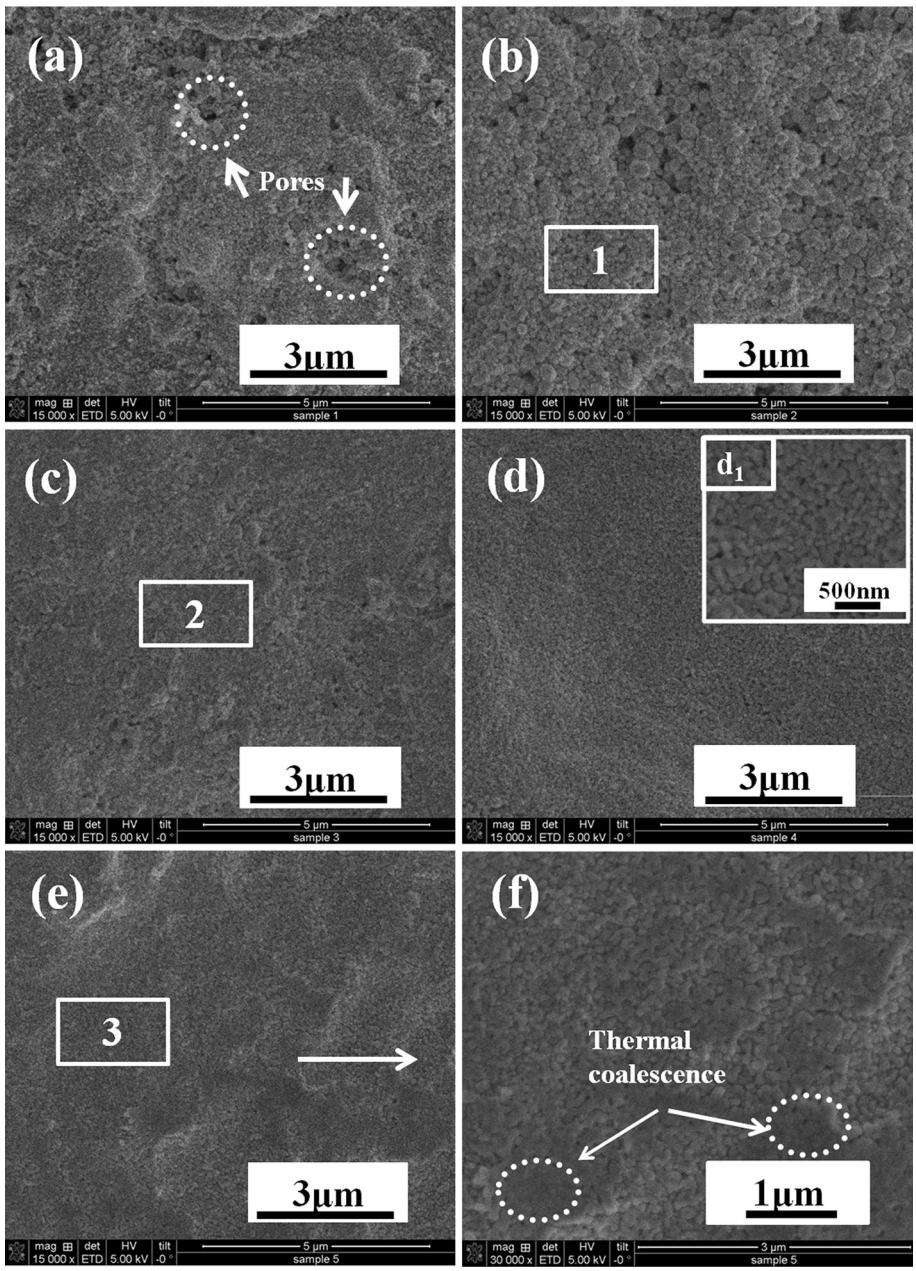

Fig. 13. SEM images of silver films sintered for 60 min at (a) 100°C, (b) 115°C, (c) 130°C, (d) 145°C, and (e) 160°C. (The inset (d1) and f are high magnification images of d and e, respectively).

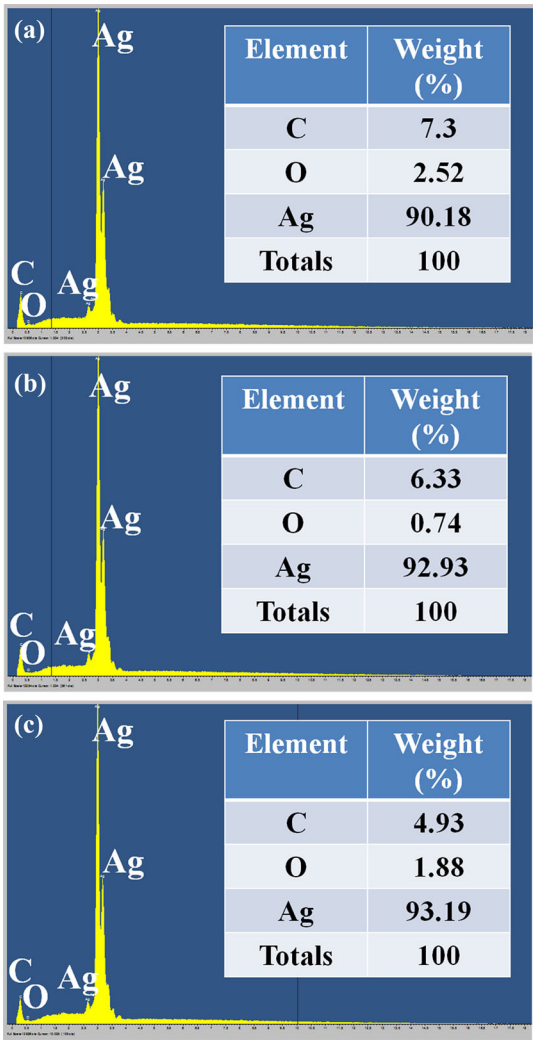

Fig. 14. EDX results in the films as a function of sintering temperature at (a) 115°C, (b) 130°C, and (c) 160°C.

Surface microstructures of silver films obtained at different temperatures were evaluated by SEM (Fig. 13). All the films show interconnected domains of silver nanoparticles. This feature is a result of fast solvent evaporation and thermal decomposition of the $[Ag(C_4H_{11}N)_2]_2C_2O_4$ complex. At lower sintering temperatures (100°C, 115°C), evaporation of the solvent component which could release bubbles is dominant because of its low boiling point and the decomposition of the complex producing silver nanoparticles is secondary. The bubbles need to go through the films consisting of silver nanoparticles, so the films are not uniform and have pores (Fig. 13a and b), though the produced silver nanoparticles could connect with each other. At sintering temperatures of 130°C and 145°C, more silver particles are produced. The films become uniform with fewer defects, the particles are homogeneous and the stacking density is increased (Fig. 13d). Sintering at higher temperature (160°C) leads to the formation of large particles

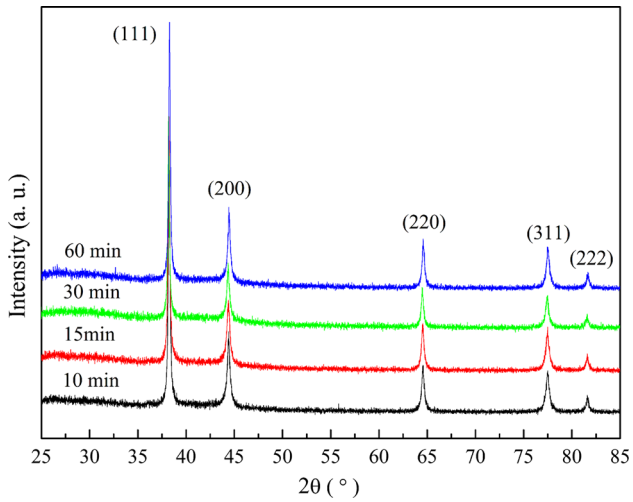

Fig. 15. XRD patterns of Ag films prepared at 130°C for 10 min, 15 min, 30 min, and 60 min, respectively.

due to the neck connection of the silver nanoparticles produced (Fig. 13f), resulting in a dense film.

Temperature plays a double role during the film formation process: (1) it aids solvent evaporation and (2) it triggers chemical reactions in the ink to produce a silver film.

The chemical composition of the silver films obtained at 115°C, 130°C, and 160°C was determined from the EDX surface energy spectra (the samples were taken from the areas 1, 2, and 3 in Fig. 13). As Fig. 14 shows, three elements (C, O, and Ag) were detected. With increasing sintering temperature, the content of Ag increased from 90.18 wt.% to 93.19 wt.% and the content of C decreased from 7.3 wt.% to 4.93 wt.%, indicating that $[Ag(C_4H_{11}N)_2]_2C_2O_4$ has almost fully decomposed to silver.

Effects of Sintering Time on Microstructure of Silver Ink Films

The effect of sintering time on the microstructure of the silver films was also studied. The samples were prepared by heating the ink on PI film at 130°C for 10 min, 15 min, 30 min, and 60 min and were characterized by XRD, SEM and EDX.

As shown in Fig. 15, silver nanocrystals could be generated within 10 min. The particle size calculated using XRD data increases as the heating time increases (Table II).

Figure 16 shows the microstructure of the silver films produced at 130°C for different times. It can be seen that the film sintered for 5 min is not uniform and there are some pores on its surface. The particles have irregular shapes and some of them seem to be covered by an organic layer (Fig. 16a). With increasing time, the films show a compact microstructure consisting of small silver particles with better film uniformity (Fig. 16b). The film

Table II. Particle size of silver nanocrystals in the films processed at 155°C for different times

Sintering time (minutes)	2θ (°)	FWHM (β)	Size (nm)
10	38.239	0.224	37.168
30	38.193	0.216	38.538
60	38.231	0.199	41.835

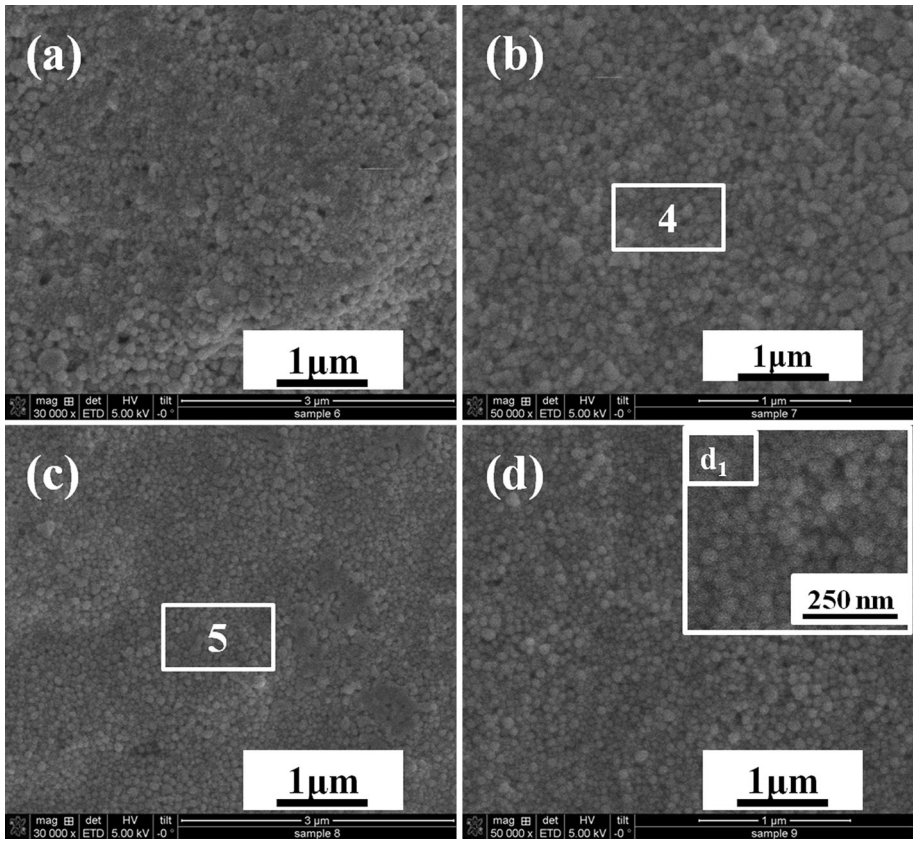

Fig. 16. SEM images of silver films produced at 130°C for 10 min, 15 min, 30 min, and 60 min (a)–(d).

sintered for 30 min has a uniform surface profile consisting of many silver particles, in contact with each other. After 60 min, a compact and uniform microstructures consisting of homogeneous spherical silver particles is formed (Fig. 16d and d_1).

The change in film morphology can be easily understood, which is related to solvent evaporation and thermal decomposition of the silver complex. When the sintering time is 5 min, solvent evaporation is inadequate, thereby resulting in an uneven film consisting of many small silver particles. For a sintering time of 15 min, the film is uniform as there is material redistribution due to decomposition of the silver complex in the film. Further increases in sintering time result in improved surface morphology.

EDX analysis was employed to investigate the changes in chemical composition, as shown in Fig. 17. The samples were taken from areas 4 and 5 of Fig. 16. As the heating time increases from 15 min to 30 min, no obvious changes in Ag and C content are observed. The results indicate that the organic molecules were decomposed and volatilized mostly within 15 min; the decomposition of the silver–amine complex continued to a large extent.

Electrical Performance

The resistivities of the silver films obtained at various temperatures were calculated from the measured sheet resistance and film thickness using the following equation (Fig. 18):

$$\rho = R_s \cdot t$$

where ρ is the resistivity, R_s the sheet resistance of the Ag film, and t the average thickness of the film which was measured to be about 1.3 ± 0.3 μm.

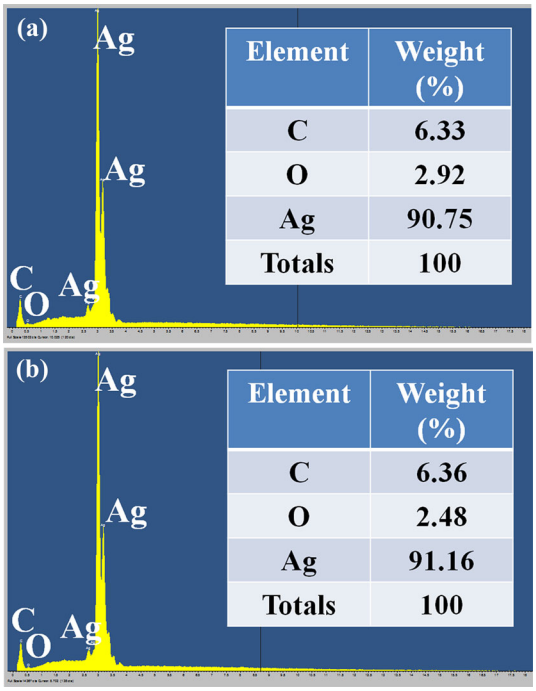

Fig. 17. EDX results of silver films produced at 130°C for (a) 15 min and (b) 30 min.

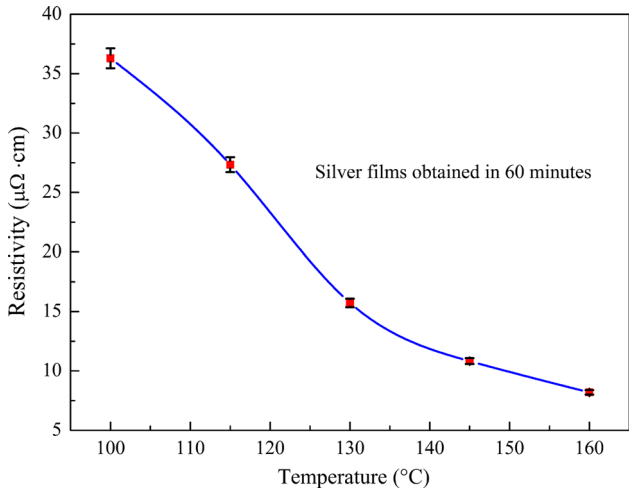

Fig. 18. Resistivity of the silver films sintered at various temperatures for 60 min.

From Fig. 18, it can be seen that the resistivity of the silver films decreases gradually as the temperature increases, from 36.29 $\mu\Omega$ cm at 100°C to 8.19 $\mu\Omega$ cm at 160°C. Below 100°C, measurements could not be carried out as the film was not totally dry and the sheet resistance was out of the measurement range of the 4-probe instrument.

At lower temperature, the solvent has partly evaporated and the formation of silver is not complete, so the resistivity is relatively high. In contrast, at higher temperatures, solvent evaporation is complete and more silver nanocrystals can be formed to improve the stacking density of Ag nanoparticles in the film, resulting in a continuous and uniform film with better particle accumulation; therefore, good film conductivity was obtained.

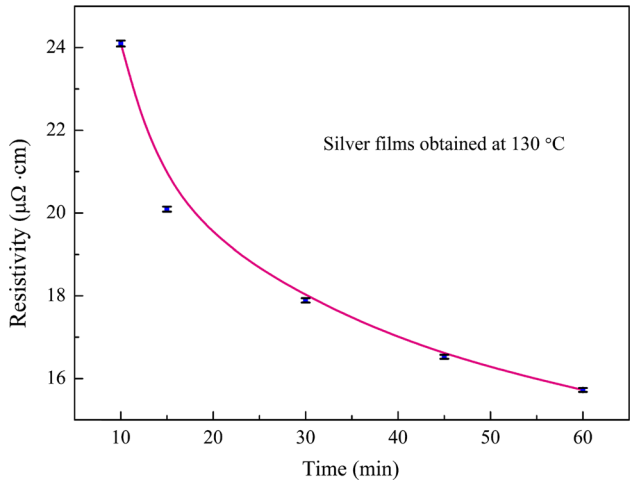

Fig. 19. Resistivity of the Ag films as a function of heating time at 130°C.

The resistivities of the films heated at 130°C for different times are shown in Fig. 19. As the sintering time increases from 5 min to 60 min, the resistivity decreases gradually from 24.10 $\mu\Omega$ cm to 15.72 $\mu\Omega$ cm. After 30 min, the improvement in resistivity is more than 37%. The decrease in resistivity with time can also be explained by the fact that more silver nanoparticles are generated, become larger and are more closely connected.

It is worth noting that film resistivity of 10^{-5} Ω cm can already be achieved at sintering temperatures around 100°C. This shows that the silver ink can be used for a variety of flexible polymer substrates such as polyethylene terephthalate.

CONCLUSIONS

In summary, a silver oxalate ink was prepared in a mixture of ethanol and ethylene glycol using the as-prepared silver oxalate as the precursor and butylamine as a complexing ligand, producing a favorable conductive film onto a PI substrate at a sintering temperature below 130°C. A silver oxalate precursor with good properties was obtained and an appropriate amine complex was formed to produce the ink. The films on PI substrates sintered at a range of temperatures and time were analyzed in terms of their morphology and resistivity, where the underlying relationship between them was demonstrated. Three factors are mainly responsible for the conductivity of the produced silver films, which are the residual level of the organic solvents, the decomposition degree of the silver–amine complex and the contact area of the silver nanoparticles.

ACKNOWLEDGEMENTS

The authors are grateful to Mr Neil Ross and Dr Jim Buckman for their assistance in the surface profilometry and EDX work respectively. Wendong Yang was supported by an EPSRC DTP studentship.

REFERENCES

1. D.W. Wang, Y. Chang, Y.X. Wang, Q. Zhang, and Z.G. Yang, *Mater. Technol. Adv. Perform. Mater.* 31, 32 (2016).
2. Y. Kim, B. Lee, S. Yang, I. Byun, I. Jeong, and S.M. Cho, *Curr. Appl. Phys.* 12, 473 (2012).
3. A.M. Jeffries, A. Mamidanna, L. Ding, O.J. Hildreth, and M.I. Bertoni, *IEEE J. Photovolt.* 7, 37 (2017).
4. J.J. Liang, K. Tong, and Q.B. Pei, *Adv. Mater.* 28, 5986 (2016).
5. J.Z. Song and H.B. Zeng, *Angew. Chem.* 54, 9760 (2015).
6. R. Dang, L.L. Song, W.J. Dong, C.R. Li, X.B. Zhang, G. Wang, and X.B. Chen, *ACS Appl. Mater. Interfaces.* 6, 622 (2014).
7. J. Yeo, G. Kim, S. Hong, M.S. Kim, D. Kim, J. Lee, H.B. Lee, J. Kwon, Y.D. Suh, H.W. Kang, H.J. Sung, J.H. Choi, W.H. Hong, J.M. Ko, S.H. Lee, S.H. Choa, and S.H. Ko, *J. Power Sources* 246, 562 (2014).
8. K. Ankireddy, A.K. Menon, B. Iezzi, S.K. Yee, M.D. Losego, and J.S. Jur, *J. Electron. Mater.* 45, 5561 (2016).
9. A. Kamyshny and S. Magdassi, *Small* 17, 3515 (2014).
10. S.B. Walker and J.A. Lewis, *J. Am. Chem. Soc.* 134, 1419 (2012).
11. R. Shankar, L. Groven, A. Amert, K.W. Whites, and J.J. Kellar, *J. Mater. Chem.* 21, 10871 (2011).
12. B.Y. Ahn, D.J. Lorang, and J.A. Lewis, *Nanoscale* 3, 2700 (2011).
13. W.D. Yang, C.Y. Liu, Z.Y. Zhang, Y. Liu, and S.D. Nie, *J. Mater. Chem.* 22, 23012 (2012).
14. Y. Chang, D.Y. Wang, Y.L. Tai, and Z.G. Yang, *J. Mater. Chem.* 22, 25296 (2012).
15. C.N. Chen, T.Y. Dong, T.C. Chang, M.C. Chen, H.L. Tsai, and W.S. Hwang, *J. Mater. Chem.* 33, 5161 (2013).
16. Q.J. Huang, W.F. Shen, and W.J. Song, *Chem. Mater.* 22, 3067 (2010).
17. Y. Dong, X.D. Li, S.H. Liu, Q. Zhu, J.G. Li, and X.D. Sun, *Thin Solid Films* 589, 381 (2015).
18. Q.J. Huang, W.F. Shen, Q.S. Xu, R.Q. Tan, and W.J. Song, *Mater. Chem. Phys.* 147, 550 (2014).
19. J.T. Wu, S.L.C. Hsu, M.H. Tsai, Y.F. Liu, and W.S. Hwang, *J. Mater. Chem.* 22, 15599 (2012).
20. D.Y. Wang, Y. Chang, Q.S. Lu, and Z.G. Yang, *Mater. Technol. Adv. Perform. Mater.* 30, 54 (2015).
21. X.L. Nie, H. Wang, and J. Zou, *Appl. Sur. Sci.* 261, 554 (2012).
22. A.L. Dearden, P.J. Smith, D.-Y. Shin, N. Reis, B. Derby, and P. O'Brien, *Macromol. Rapid Commun.* 26, 315 (2005).
23. S.F. Jahn, T. Blaudeck, R.R. Baumann, A. Jakob, P. Ecorchard, T. Ruffer, H. Lang, and P. Schmidt, *Chem. Mater.* 22, 3067 (2010).
24. K. Black, S. Jetinder, M. Danielle, S. Sarah, J.C. Sutcliffe, and R.P. Paul, *Sci. Rep.* 6, 1 (2016).
25. Y. Tao, B. Wang, L. Wang, and Y. Tai, *Nanoscale Res. Lett.* 8, 1 (2013).
26. Y. Dong, X. Li, S. Liu, Q. Zhu, M. Zhang, J.G. Li, and X. Sun, *Thin Solid Films* 616, 635 (2016).
27. V.V. Boldyrev, *Thermochim. Acta* 388, 63 (2002).
28. K. Zope, Novel synthesis of a solid silver oxalate complex used for printing conductive traces. Thesis of Rochester Institue of Technology (2017), http://scholarworks.rit.edu/theses/9381. Accessed 11 Jan 2017.
29. G. Corro, U. Pal, E. Ayala, and E. Vidal, *Catal. Today* 212, 63 (2013).